AFRL-HE-BR-TR-2002-0155

UNITED STATES AIR FORCE RESEARCH LABORATORY

DIELECTRIC RESPONSE DATA ON MATERIALS OF MILITARY CONSEQUENCE

Richard Medina
John Penn
Richard Albanese

HUMAN EFFECTIVENESS DIRECTORATE
DIRECTED ENERGY BIOEFFECTS DIVISION
BIOMECHANISMS AND MODELING BRANCH
2503 Gillingham Dr.
Brooks AFB, Texas 78235

August 2002

Approved for public release; distribution unlimited.

NOTICES

This report is published in the interest of scientific and technical information exchange and does not constitute approval or disapproval of its ideas or findings.

This report is published as received and has not been edited by the publication staff of the Air Force Research Laboratory.

Using Government drawings, specifications, or other data included in this document for any purpose other than Government-related procurement does not in any way obligate the US Government. The fact that the Government formulated or supplied the drawings, specifications, or other data, does not license the holder or any other person or corporation, or convey any rights or permission to manufacture, use, or sell any patented invention that may relate to them.

The Office of Public Affairs has reviewed this paper, and it is releasable to the National Technical Information Service, where it will be available to the general public, including foreign nationals.

This report has been reviewed and is approved for publication.

Richard A. Albanese, M

RICHARD A. ALBANESE, M. D.
Contract Monitor

RMiller

RICHARD L. MILLER, Ph.D.
Chief, Directed Energy Bioeffects Division

REPORT DOCUMENTATION PAGE

Form Approved
OMB No. 0704-0188

1. REPORT DATE *(DD-MM-YYYY)*	2. REPORT TYPE	3. DATES COVERED *(From - To)*
31 July 2002	Final	1999-2002

4. TITLE AND SUBTITLE
Dielectric Response Data on Materials of Military Consequence

5a. CONTRACT NUMBER

5b. GRANT NUMBER

5c. PROGRAM ELEMENT NUMBER
62202F

6. AUTHOR(S)
Medina, Richard L., Penn, John W., Albanese, Richard A.

5d. PROJECT NUMBER
7757

5e. TASK NUMBER
B4

5f. WORK UNIT NUMBER
07

7. PERFORMING ORGANIZATION NAME(S) AND ADDRESS(ES)
Air Force Research Laboratorv
Human Effectiveness Directorate
Directed Energy Bioeffects Division
Biomechanisms and Modeling Branch
2503 Gillingham Drive
Brooks AFB TX 78235-5102

8. PERFORMING ORGANIZATION REPORT NUMBER
AFRL-HE-BR-TR-2002-0155

9. SPONSORING / MONITORING AGENCY NAME(S) AND ADDRESS(ES

10. SPONSOR/MONITOR'S ACRONYM(S)

11. SPONSOR/MONITOR'S REPORT NUMBER(S)

12. DISTRIBUTION / AVAILABILITY STATEMENT
Approved for public release; distribution unlimited.

13. SUPPLEMENTARY NOTES

14. ABSTRACT
We are interested in the remote determination of materials. That is, we desire to irradiate a material from a distance using efficient antenna systems and infer from the scattered signal the nature of the irradiated material. To accomplish this task we require a library of material properties as related to electromagnetic scattering and we require signal features that permit materials to be discriminated from a distance using scattered signals. This technical report provides a significant first step in the direction of providing the needed capability. A small materials library is presented along with signal properties of interest.

15. SUBJECT TERMS
remote sensing, materials identification, dispersive properties

16. SECURITY CLASSIFICATION OF:			17. LIMITATION OF ABSTRACT	18. NUMBER OF PAGES	19a. NAME OF RESPONSIBLE PERSON
					Dr. Richard Albanese
a. REPORT	b. ABSTRACT	c. THIS PAGE			19b. TELEPHONE NUMBER *(include area code)*
Unclass	Unclass	Unclass	Unclass	32	(210) 536-5710

Dielectric Response Data on Materials of Military Consequence

Richard L Medina, John W Penn and Richard A Albanese
Biomechanisms and Modeling Branch
Human Effectiveness Directorate
Air Force Research Laboratory
Brooks AFB, San Antonio, Texas 78235

1 Introduction

The ultimate goal of this report is to make accurate determinations of the relative dielectric value and conductivity of materials from scattering measurements. We have identified steel, concrete, foliage, soil, wood, cardboard, and plastic as materials of potential military consequence. In this report, we used the following definitions for relative dielectric value as $\varepsilon=\varepsilon'/\varepsilon_0$ and conductivity as $\sigma=\omega\varepsilon''\varepsilon_0$ as described in reference (1). The parameters ε',ε'',ω and ε_0 are defined in section 2.

The permittivity data came from open literature articles and books. We discovered early that permittivity data for materials occurs in a wide variety of journals and books and is usually collected for specific frequencies of interest. The most current articles have made an effort to report temperature, moisture content by weight, and composition of material.

To predict material response signatures, we first solve the direct problem. The direct problem consists of calculating electromagnetic fields occurring within the material due to exposure to external sources. Both the calculation of internal fields and the optimal selection of external sources require the exact determination of the electrical coefficients of the materials as functions of frequency, moisture content and temperature. Some knowledge of the relative dielectric value and conductivity for these materials is available, but this knowledge appears to be limited with respect to desired frequencies.

This report describes the detailed steps taken to compute materials response signatures. Relative dielectric value and conductivity data were collected for each of the selected media. Section 2 of this report describes the least-square routine used to fit the available data. Next in section 3, we show fitted equations for each material and data values plotted by frequency for relative dielectric value and conductivity. In section 4 we solve the direct problem. The response of a 2.1 GHz plane-wave modulated pulse train irradiating each of the materials of interest is investigated. Signature plots taken at a depth of 1.88 meters are generated, and waveform velocities are calculated for each material. In section 5 we discuss follow-up work.

The permittivity data collected will permit us to predict material signatures at a given depth within the material. The data is valuable because it also allows us to study both the direct and inverse problems for the identification of materials.

2 Fitting Procedure

A computer program written by William D Hurt at the Directed Energy Bioeffects Division, Human Effectiveness Directorate, AFRL was used to fit available data to Debye curves of one or more compartments (or number of terms of the equations described below). For a given material, measured values of relative dielectric value and conductivity at various frequencies are needed along with estimates of the high frequency dielectric value asymptote and number of compartments. The number of compartments is determined by the internal structure of the material, and may be estimated from the bends in a plot of relative dielectric value against frequency.

An important feature of the fitting program is that for lossy materials, that is, materials with conductivity, the program properly considers the correct inherent dependence of the relative dielectric value and conductivity of the complex permittivity function on frequency. This formulation is based on certain assumptions that satisfy Maxwell's equations. Failure to consider this dependence causes the apparent response of the material to appear before the true response of the material (non- causal behavior).

The fitting program computes a least-square fit of the low frequency conductivity and, for each compartment, the dielectric value contribution and the relaxation time for the material. The complex permittivity model is written as $\varepsilon^* = \varepsilon' - i\varepsilon''$ where ε' represents the reactive property of the material and ε'' represents the resistive property of a linear material as a function of frequency (1). In our report, we will use the symbol ε to represent the relative dielectric value ($\varepsilon=\varepsilon'/\varepsilon_0$) of the material and the symbol σ to represent conductivity ($\sigma=\omega\varepsilon''\varepsilon_0$). From reference (2), we see that the relative dielectric value and conductivity can be expressed as

$$\varepsilon = \varepsilon_\infty + \sum_{j=1}^{n} \frac{\Delta_j}{1+\left(\dfrac{\omega}{\omega_j}\right)^2}$$

and

$$\sigma = \sigma_0 + \omega^2 \varepsilon_0 \sum_{j=1}^{n} \frac{\dfrac{\Delta_j}{\omega_j}}{1+\left(\dfrac{\omega}{\omega_j}\right)^2}$$

where ε_∞ is the high frequency dielectric value asymptote, σ_o is the limit of the conductivity as $\omega \rightarrow 0$, $\varepsilon_0 = 8.85*10^{-12}$ F/m, Δ_j is the change in the relativity dielectric value due to the dispersion associated with $\omega_j=2\pi f_j$ and f_j is the dispersion frequency. The least-square fitting program estimates jointly ε and σ using a weighted leastsquares error metric. A detailed explanation of how this is accomplished can be found in the reference (2).

The equations computed by this method will give very accurate estimates of relative dielectric value and conductivity over the frequency range 10 Hertz – 100GigaHertz if measured values of sufficient number, frequency range and accuracy are available. For many of the materials studied here, the published points fail to meet these conditions. However, the computed material parameters should be accurate within the sample variability.

We have computed electrical properties for the available points only. Additional points or estimated values at critical frequencies could make our results more realistic.

We have selected the number of compartments for each material by selecting the best sum of squares residuals fit from several trials.

3 Fitting Results

Each material class had numerous variations of composition, temperature and/or moisture content. For this report, we chose one material variation to represent each class. The material data values collected from the literature and used in this report can be found in the appendix A.

For each material, we provide the relative dielectric value and conductivity (Siemens/meter) fitting equation. We also provide plots of each material fit as a solid line against the material data values obtained from the literature plotted as asterisks.

The first material we consider is steel. This is essentially a non-dispersive material with an approximate relative dielectric value of 1 and conductivity of $0.5*10^7$ at 20 degrees centigrade for the range of frequencies of interest in this report (3). Since this material is non-dispersive no plot is shown.

The concrete data chosen for this report is Cenco Sealstix cement at 23 degrees centigrade and unknown moisture content (4). The result of a least-square fit is a four-compartment model. The computed dielectric value sum of squares (SSQ) residual is 0.00223 and conductivity SSQ residual is 0.00001 for seven data values. Relative dielectric value and conductivity (Siemens/meter) fitting equations are

$$\varepsilon = 2.9 + \frac{3.0936\cdot10^{-1}}{1+\left(\frac{f_{Ghz}}{3.9686\cdot10^{-7}}\right)^2} + \frac{2.7072\cdot10^{-1}}{1+\left(\frac{f_{Ghz}}{2.8872\cdot10^{-5}}\right)^2} + \frac{2.6680\cdot10^{-1}}{1+\left(\frac{f_{Ghz}}{3.5521\cdot10^{-3}}\right)^2} + \frac{1.5275\cdot10^{-1}}{1+\left(\frac{f_{Ghz}}{5.8733}\right)^2}$$

$$\sigma = 5.6751\cdot10^{-10} + \frac{4.3367\cdot10^{4}\cdot f_{Ghz}^2}{1+\left(\frac{f_{Ghz}}{3.9686\cdot10^{-7}}\right)^2} + \frac{5.2165\cdot10^{2}\cdot f_{Ghz}^2}{1+\left(\frac{f_{Ghz}}{2.8872\cdot10^{-5}}\right)^2} + \frac{4.1785\cdot f_{Ghz}^2}{1+\left(\frac{f_{Ghz}}{3.5521\cdot10^{-3}}\right)^2} + \frac{1.4468\cdot10^{-3}\cdot f_{Ghz}^2}{1+\left(\frac{f_{Ghz}}{5.8733}\right)^2}$$

Figures 1a and 1b provide the relative dielectric value and conductivity plots for Cenco Sealstix cement. (In section 4, signature response for each of the materials will be predicted.)

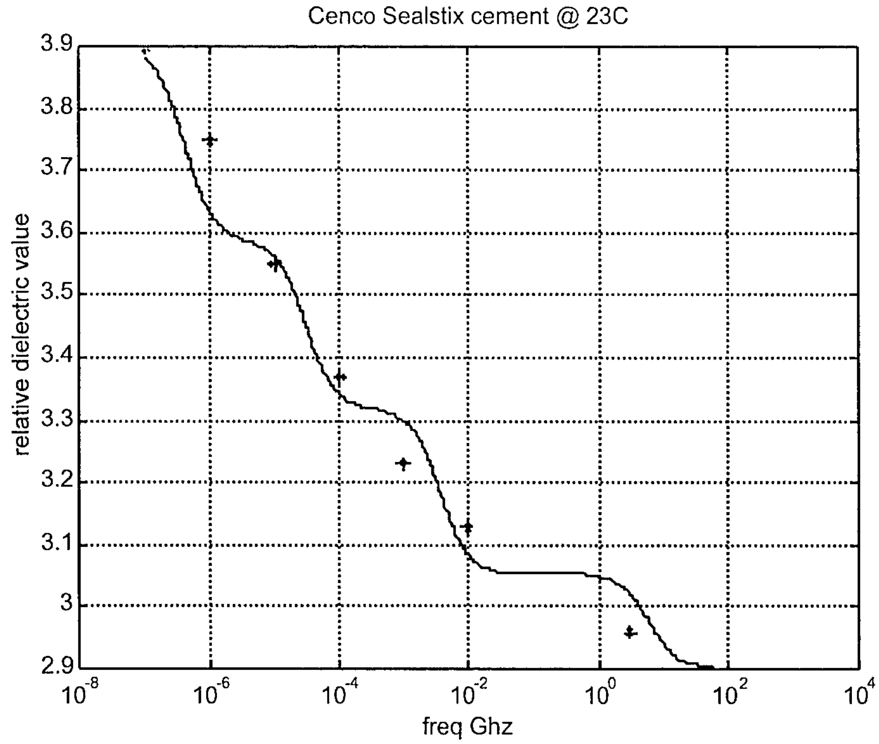

Figure 1a. Cenco Sealstix cement relative dielectric value data (asterisk) plotted against least-square fit(solid line).

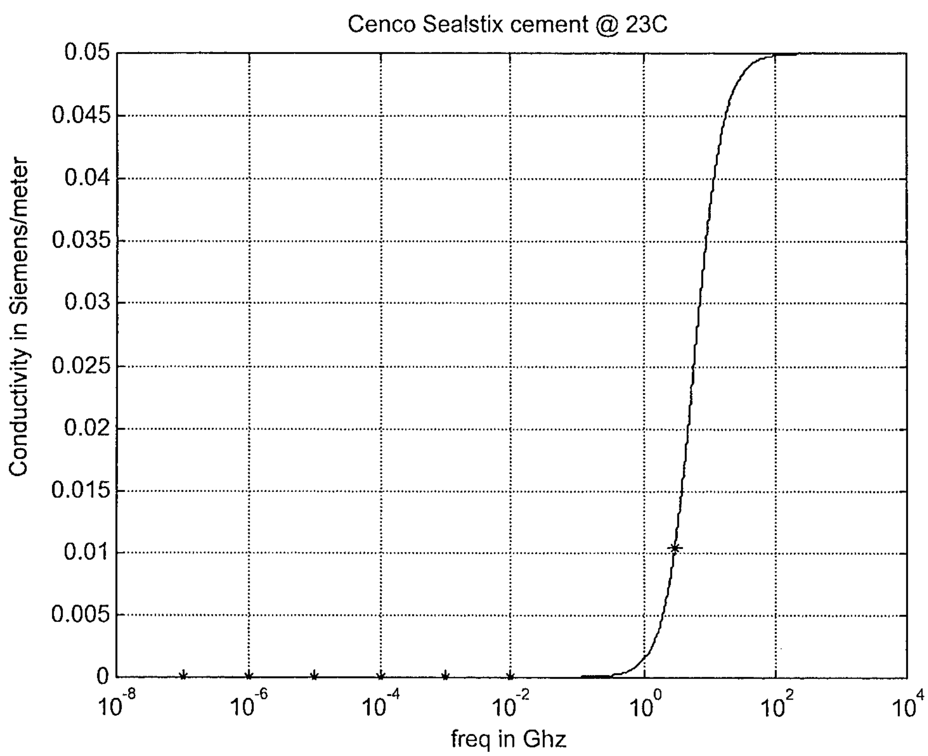

Figure 1b. Cenco Sealstix cement conductivity data (asterisk) plotted against least-square fit(solid line).

Foliage is made up of many biological components such as leaves, branches, and tree trunks. To understand foliage we studied various components of vegetation such as tree trunks, stems and leaves (7). A complex permittivity leaf model developed by Fung and Ulaby in 1978 (5) was used for this report. We believe this model characterizes dense tree canopies as seen from above. Fung and Ulaby defined the complex permittivity of a single leaf as

$$\varepsilon_{leaf} = \varepsilon_r - j\varepsilon_i$$

where

$$\varepsilon_r = 5.5 + \frac{\varepsilon_m - 5.5}{1 + f^2\tau^2}$$

$$\varepsilon_i = (\varepsilon_m - 5.5)\frac{f\tau}{1 + f^2\tau^2}$$

$$\varepsilon_m = 5 + 51.56 \cdot V_W$$

ε_r is then our relative dielectric value, $\varepsilon_i = \sigma/(\omega\varepsilon_o)$ and ε_m is defined as relative macroscopic static permittivity. The parameter V_w is a volume-filling factor of the dispersed water granules and is set at 0.35 to provide moisture content of 35% by weight. The parameter τ is the relaxation time of water and is set at $6.167 * 10^{-11}$ for temperature of 20 degrees centigrade. Figures 2a and 2b provide the relative dielectric value and conductivity plots for this model. Fung and Ulaby did not provide the raw data for their curve fit.

The equations above approximate the electrical properties of a volume of solid leaf material. A foliage canopy will consist of mostly air between leaves. Currently, we are looking for measured data to enable us to adjust these equations to realistic conditions.

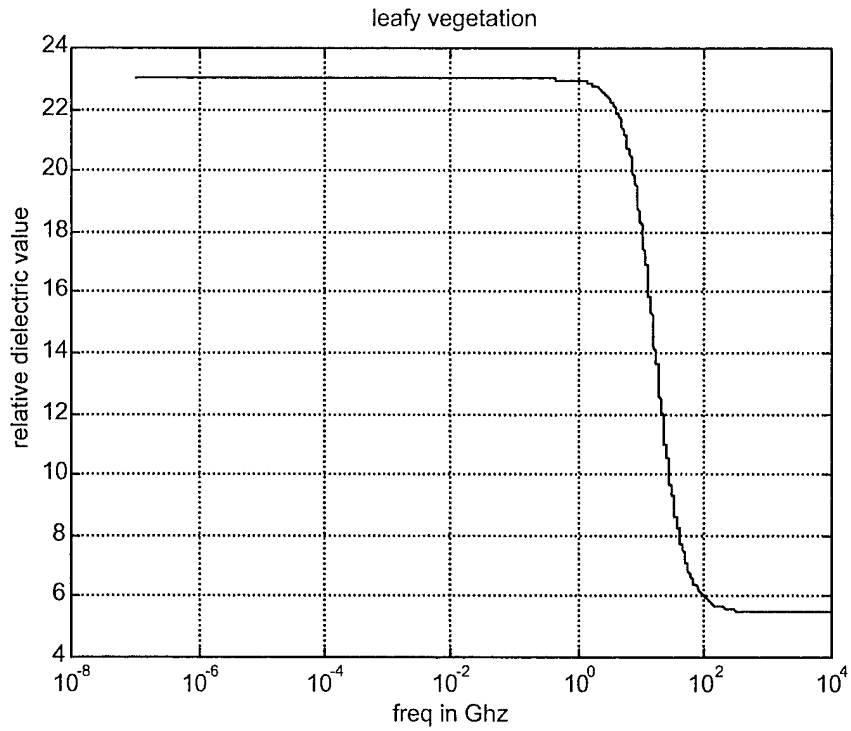

Figure 2a. Single leaf foliage relative dielectric value model developed by Fung and Ulaby in 1978.

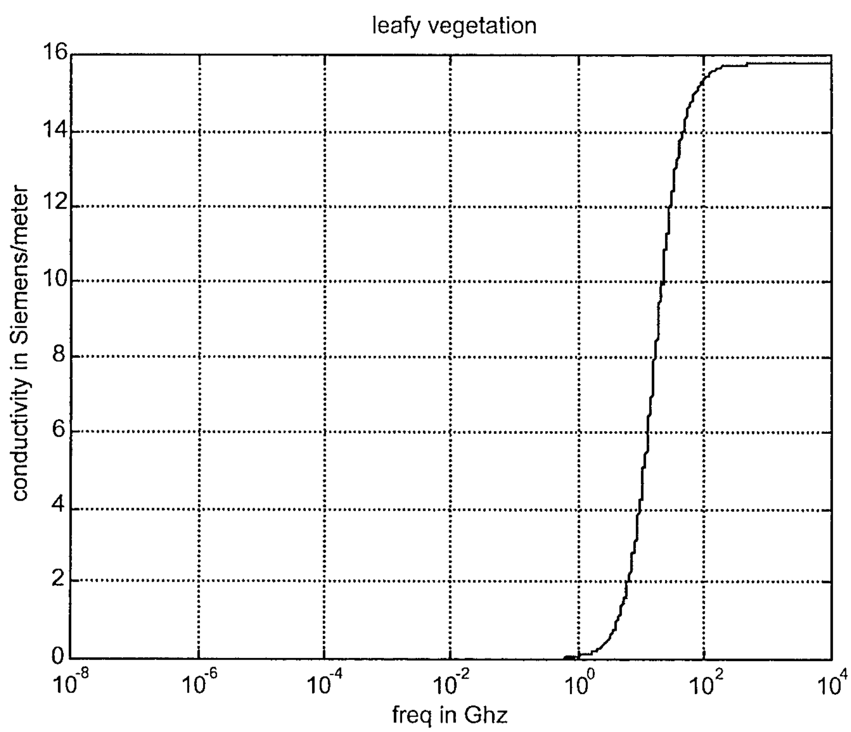

Figure 2b. Single leaf foliage conductivity model developed by Fung and Ulaby in 1978.

There are several different types of soils with varying moisture content, temperature and composition. We choose loamy soil for this report because it may be a soil composition typical of Bosnia. We have 2.2% and 0.0% moisture content loamy soil at a temperature of 25 degrees centigrade (6). For loamy soil with 2.2% moisture by weight content, the result of a least-square fit is a three-compartment model with dielectric value SSQ residual of 0.15900 and conductivity SSQ residual of 0.05932 for six data values. Relative dielectric value and conductivity (Siemens/meter) fitting equations are

$$\varepsilon = 3.45 + \frac{1.2378 \cdot 10^{1}}{1+\left(\frac{f_{Ghz}}{3.7748 \cdot 10^{-4}}\right)^2} + \frac{2.3981}{1+\left(\frac{f_{Ghz}}{1.6699 \cdot 10^{-2}}\right)^2} + \frac{2.6857 \cdot 10^{-1}}{1+\left(\frac{f_{Ghz}}{4.3171}\right)^2}$$

$$\sigma = 1.5882 \cdot 10^{-5} + \frac{1.8243 \cdot 10^{3} \cdot f_{Ghz}^2}{1+\left(\frac{f_{Ghz}}{3.7748 \cdot 10^{-4}}\right)^2} + \frac{7.9889 \cdot f_{Ghz}^2}{1+\left(\frac{f_{Ghz}}{1.6699 \cdot 10^{-2}}\right)^2} + \frac{3.4609 \cdot 10^{-3} \cdot f_{Ghz}^2}{1+\left(\frac{f_{Ghz}}{4.3172}\right)^2}$$

For loamy soil with 0.0% moisture content, the result of a least-square fit is a three-compartment model with SSQ residuals for dielectric value of 0.00271 and SSQ residuals for conductivity of 0.00001 for seven data values. Relative dielectric value and conductivity (Siemens/meter) fitting equations are

$$\varepsilon = 2.4 + \frac{1.8984 \cdot 10^{-1}}{1+\left(\frac{f_{Ghz}}{2.3215 \cdot 10^{-4}}\right)^2} + \frac{1.2471 \cdot 10^{-1}}{1+\left(\frac{f_{Ghz}}{3.8361 \cdot 10^{-2}}\right)^2} + \frac{6.1010 \cdot 10^{-3}}{1+\left(\frac{f_{Ghz}}{1.3517 \cdot 10^{1}}\right)^2}$$

$$\sigma = 4.7744 \cdot 10^{-8} + \frac{4.5494 \cdot 10^{1} \cdot f_{Ghz}^2}{1+\left(\frac{f_{Ghz}}{2.3215 \cdot 10^{-4}}\right)^2} + \frac{1.8086 \cdot 10^{-1} \cdot f_{Ghz}^2}{1+\left(\frac{f_{Ghz}}{3.8361 \cdot 10^{-2}}\right)^2} + \frac{2.5110 \cdot 10^{-5} \cdot f_{Ghz}^2}{1+\left(\frac{f_{Ghz}}{1.3517 \cdot 10^{1}}\right)^2}$$

Figures 3a and 3b show loamy soil at 2.2% moisture content and figures 4a and 4b show loamy soil for 0.0% moisture content.

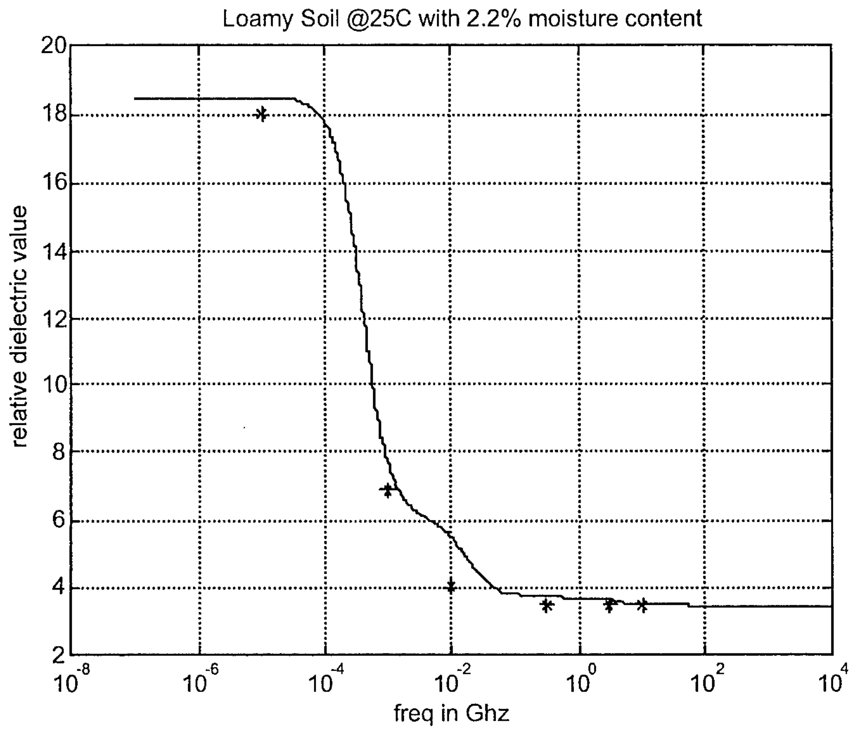

Figure 3a. Loamy soil relative dielectric value data (asterisk) plotted against least-square (solid line) with 2.2% moisture content.

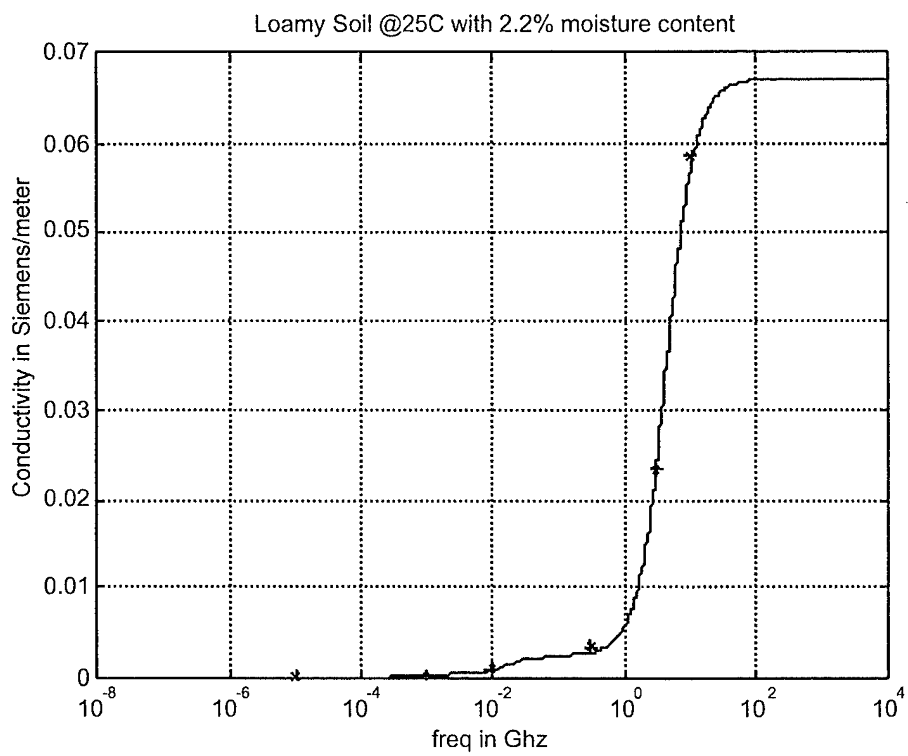

Figure 3b. Loamy soil conductivity data (asterisk) plotted against least-square (solid line) with 2.2% moisture content.

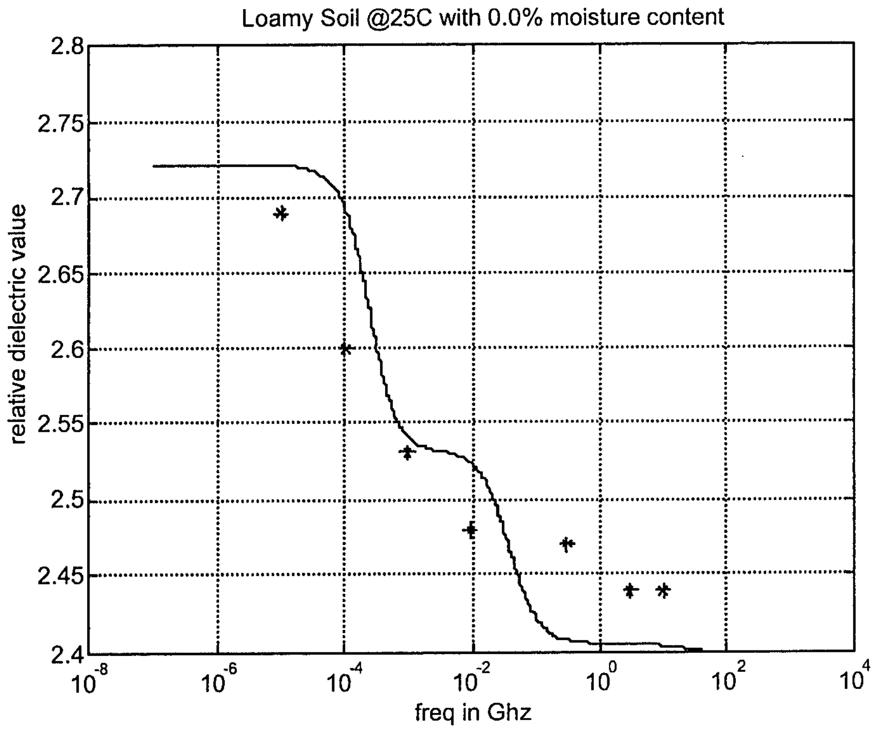

Figure 4a. Loamy soil relative dielectric value data (asterisk) plotted against least-square with 0.0% moisture content (dry basis).

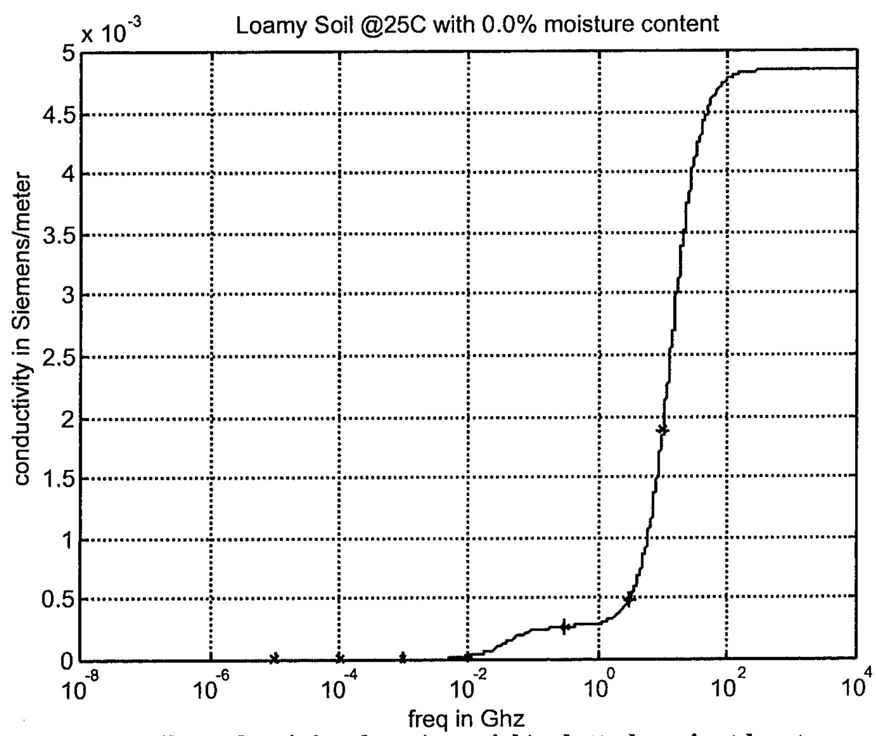

Figure 4b. Loamy soil conductivity data (asterisk) plotted against least-square with 0.0% moisture content (dry basis).

Wood is the next material of interest because it is possible to use in the construction of decoy targets to confuse airborne or ground surveillance (4). The wood we chose was Douglas Fir Plywood at 25 degrees centigrade and unknown moisture content. The result of a least-square fit is a three-compartment model with dielectric value SSQ residual of 0.01071 and conductivity SSQ residual of 1.16019 for eight data values. Relative dielectric value and conductivity (Siemens/meter) fitting equations are

$$\varepsilon = 1.55 + \frac{1.1022 \cdot 10^{-1}}{1+\left(\dfrac{f_{Ghz}}{3.5310 \cdot 10^{-5}}\right)^2} + \frac{3.4566 \cdot 10^{-1}}{1+\left(\dfrac{f_{Ghz}}{5.3192 \cdot 10^{-2}}\right)^2} + \frac{6.8760 \cdot 10^{-2}}{1+\left(\dfrac{f_{Ghz}}{2.5017 \cdot 10^{1}}\right)^2}$$

$$\sigma = 1.4340 \cdot 10^{-10} + \frac{1.7366 \cdot 10^{2} \cdot f_{Ghz}^2}{1+\left(\dfrac{f_{Ghz}}{3.5310 \cdot 10^{-5}}\right)^2} + \frac{3.6151 \cdot 10^{-1} \cdot f_{Ghz}^2}{1+\left(\dfrac{f_{Ghz}}{5.3192 \cdot 10^{-2}}\right)^2} + \frac{1.5291 \cdot 10^{-4} \cdot f_{Ghz}^2}{1+\left(\dfrac{f_{Ghz}}{2.5017 \cdot 10^{1}}\right)^2}$$

Figures 5a and 5b show the relative dielectric value and conductivity plots for Douglas Fir Plywood.

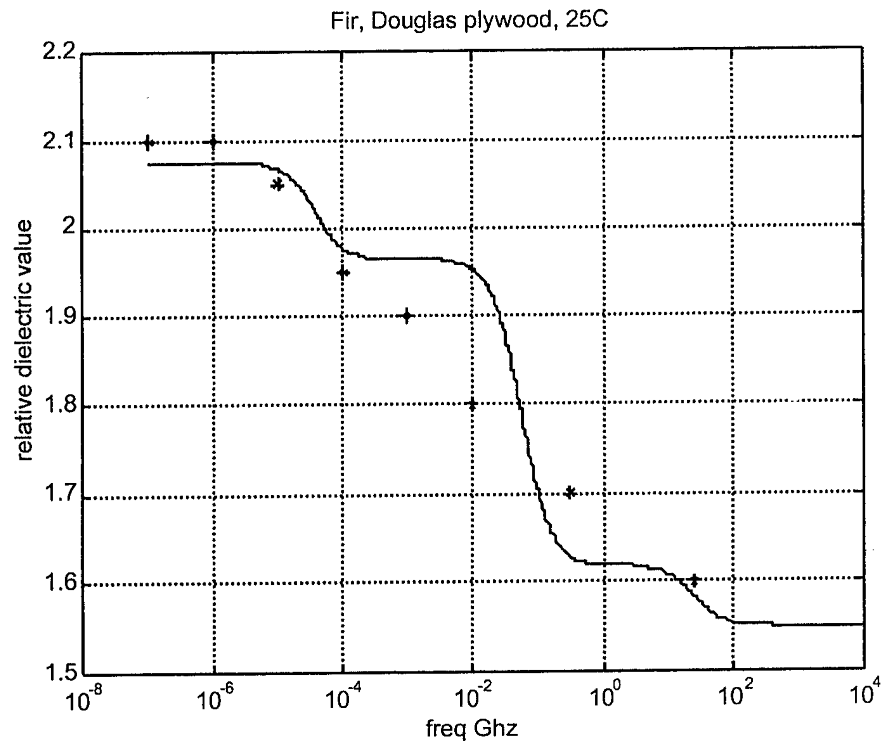

Figure 5a. Fir Douglas plywood relative dielectric value data (asterisk) plotted against least-square fit (solid line).

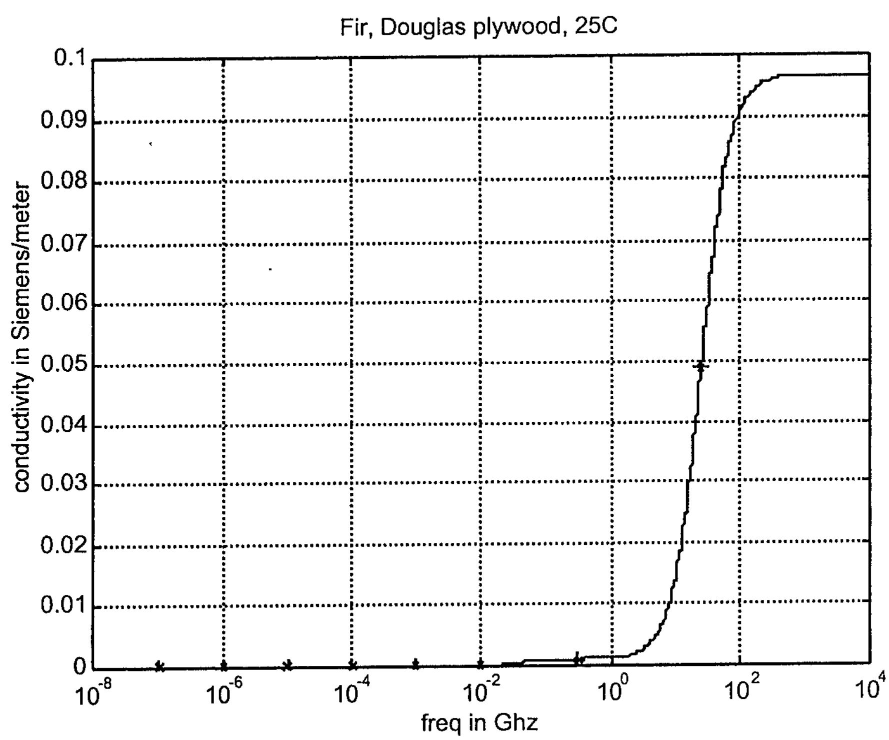

Figure 5b. Fir Douglas plywood conductivity data (asterisk) plotted against least-square fit (solid line).

Another material of interest is cardboard which is a composition of pressed paper pulp and glue. An approximate cardboard material is Royalgrey paper at 25 degrees centigrade and unknown moisture content (4). The result of a least-square fit is a four-compartment model with dielectric value SSQ residual of 0.06831 and conductivity SSQ residual of 0.22582 for ten data values. Relative dielectric value and conductivity (Siemens/meter) fitting equations are

$$\varepsilon = 2.3 + \frac{9.4035\cdot 10^{-2}}{1+\left(\frac{f_{Ghz}}{3.8241\cdot 10^{-6}}\right)^2} + \frac{2.6185\cdot 10^{-1}}{1+\left(\frac{f_{Ghz}}{4.4366\cdot 10^{-4}}\right)^2} + \frac{5.7978\cdot 10^{-1}}{1+\left(\frac{f_{Ghz}}{3.9638\cdot 10^{-2}}\right)^2} + \frac{3.1151\cdot 10^{-1}}{1+\left(\frac{f_{Ghz}}{3.5267}\right)^2}$$

$$\sigma = 9.2490\cdot 10^{-11} + \frac{1.3680\cdot 10^{3}\cdot f_{Ghz}^2}{1+\left(\frac{f_{Ghz}}{3.8241\cdot 10^{-6}}\right)^2} + \frac{3.2835\cdot 10^{1}\cdot f_{Ghz}^2}{1+\left(\frac{f_{Ghz}}{4.4366\cdot 10^{-4}}\right)^2} + \frac{8.1374\cdot 10^{-1}\cdot f_{Ghz}^2}{1+\left(\frac{f_{GHz}}{3.9638\cdot 10^{-2}}\right)^2} + \frac{4.9140\cdot 10^{-3}\cdot f_{Ghz}^2}{1+\left(\frac{f_{Ghz}}{3.5267}\right)^2}$$

Figures 6a and 6b show the relative dielectric value and conductivity plots for Royalgrey paper.

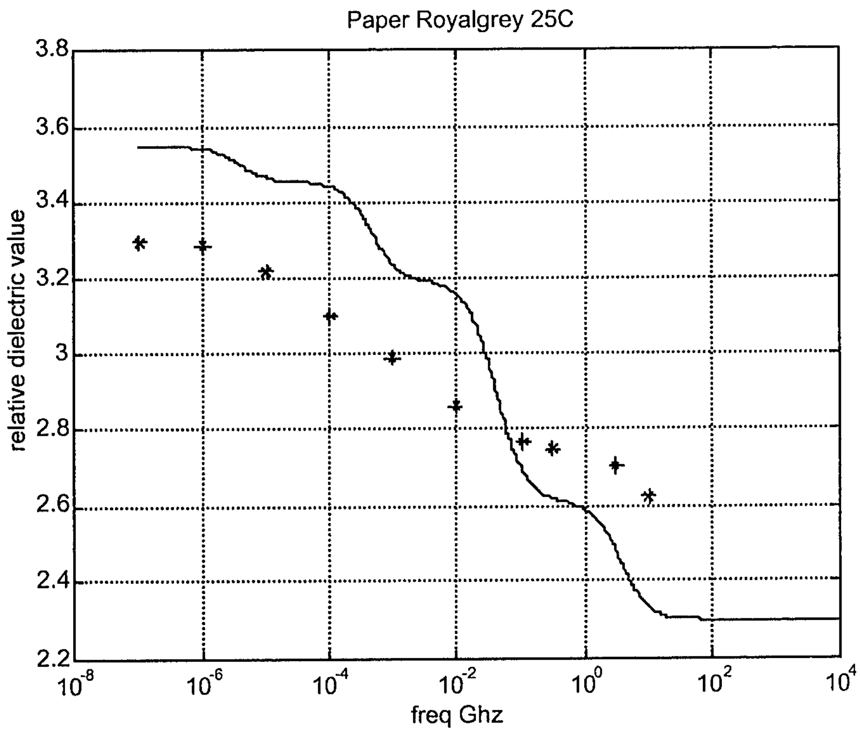

Figure 6a. Royalgrey paper relative dielectric value data (asterisk) plotted against least-square fit (solid line).

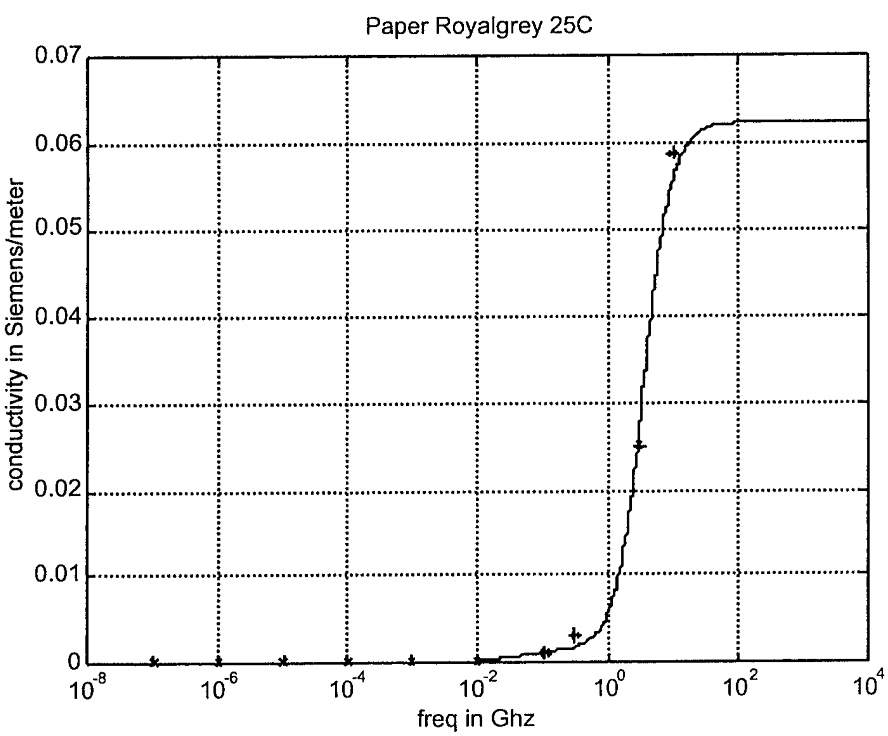

Figure 6b Royalgrey paper conductivity data (asterisk) plotted against least-square fit (solid line).

The last material is polyvinyl chloride, a plastic material. We chose a plastic called Lucite because of its commercial popularity (4). The interest in plastics involves land mines, pipes, automobile bodies and organic coatings such as paints and varnishes. The result of a least-square fit is a five-compartment model with dielectric value SSQ residual of 0.00029 and conductivity SSQ residual of 0.23271 for eleven data values. Relative dielectric value and conductivity (Siemens/meter) fitting equations are

$$\varepsilon = 2.55 + \frac{2.7781\cdot 10^{-1}}{1+\left(\dfrac{f_{Ghz}}{3.7410\cdot 10^{-7}}\right)^2} + \frac{1.4256\cdot 10^{-1}}{1+\left(\dfrac{f_{Ghz}}{6.4603\cdot 10^{-6}}\right)^2} + \frac{1.3665\cdot 10^{-1}}{1+\left(\dfrac{f_{Ghz}}{2.7057\cdot 10^{-4}}\right)^2}$$

$$+ \frac{6.3914\cdot 10^{-2}}{1+\left(\dfrac{f_{Ghz}}{2.9875\cdot 10^{-2}}\right)^2} + \frac{2.7811\cdot 10^{-2}}{1+\left(\dfrac{f_{Ghz}}{5.1161}\right)^2}$$

$$\sigma = 5.9263\cdot 10^{-10} + \frac{4.1303\cdot 10^{4}\cdot f_{Ghz}^2}{1+\left(\dfrac{f_{Ghz}}{3.7419\cdot 10^{-7}}\right)^2} + \frac{1.2276\cdot 10^{3}\cdot f_{Ghz}^2}{1+\left(\dfrac{f_{Ghz}}{6.4603\cdot 10^{-6}}\right)^2} + \frac{2.8097\cdot 10^{1}\cdot f_{Ghz}^2}{1+\left(\dfrac{f_{Ghz}}{2.7057\cdot 10^{-4}}\right)^2}$$

$$+ \frac{1.1902\cdot 10^{-1}\cdot f_{Ghz}^2}{1+\left(\dfrac{f_{Ghz}}{2.9875\cdot 10^{-2}}\right)^2} + \frac{3.0242\cdot 10^{-4}\cdot f_{Ghz}^2}{1+\left(\dfrac{f_{Ghz}}{5.1161}\right)^2}$$

Figures 7a and 7b provide the relative dielectric value and conductivity plots for Lucite HM-122 plastic at 25 degrees centigrade.

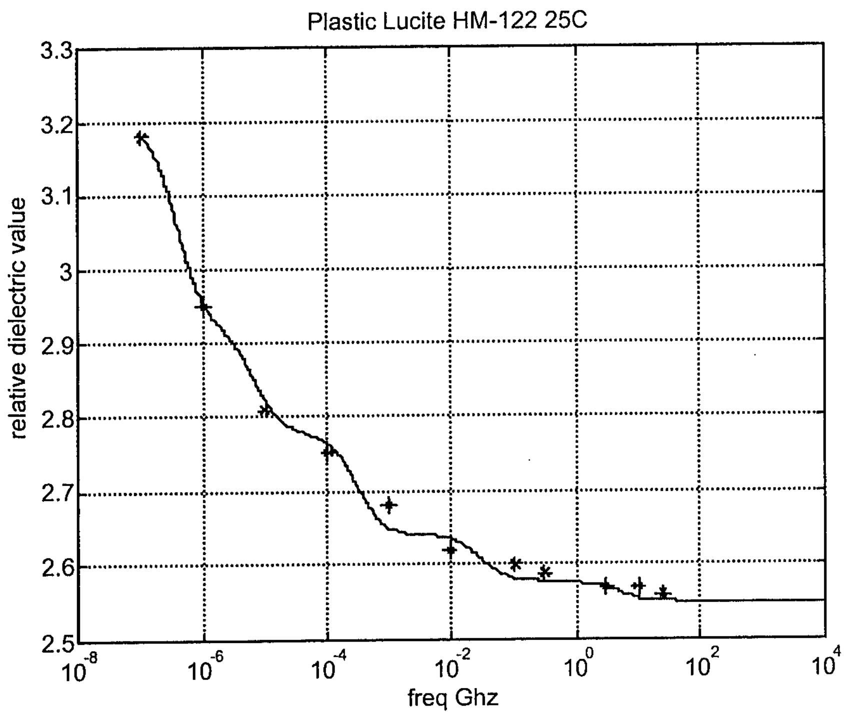

Figure 7a. Plastic Lucite HM-122 relative dielectric value data (asterisk) plotted against least-square fit (solid line).

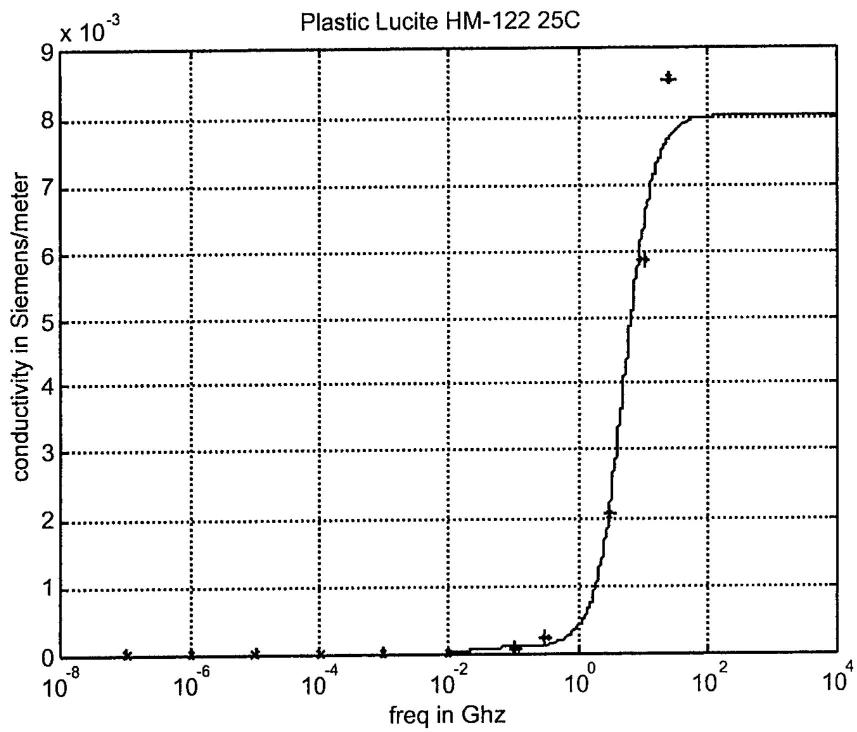

Figure 7b. Plastic Lucite HM-122 conductivity data (asterisk) plotted against least-square fit (solid line).

4. Material signature response.

In this section we will examine the signature response of a plane wave pulse train irradiating a homogeneous material half-space model and how distinct this signature is from that of other materials. We pay particular attention to the effects of the dielectric dispersive properties of each material on the pulse-train propagation. The half-space geometry shown in figure 8 is used in this study.

The irradiating source is a square-wave modulated sinusoid pulse with frequency 2.1 GHz. The total pulse event duration is 10 cycles for a duration time of 4.7619 nanoseconds and 10 cycles off for a period of 9.5238 nanoseconds. A square-wave modulated sinusoid oscillating at 2.1 GHz is shown in Figure 9. Calculations are made at a depth of 1.88 meter into the medium.

If the propagation path is through a vacuum, the velocity of the a square-wave modulated sinusoid pulse can be calculated by the following equation

$$c = \frac{1}{\sqrt{\varepsilon_o \mu_o}} = 2.998 \cdot 10^8 m/\sec \approx 3 \cdot 10^8 m/\sec$$

where ε_0=8.854*10^{-12} F/m and μ_0=1.257*10^{-6} H/m are free space constants. An approximate velocity of an electromagnetic wave in a medium can be calculated using the following equation (conductivity effects have been neglected):

$$v_{medium} \approx \frac{c}{\sqrt{\varepsilon_{relative\,dielectric\ value\ of\ medium}}} m/\sec$$

where $\varepsilon_{\text{relative dielectric value}}$ of medium at 2.1 GHz (8). We have provided a tabular list of electromagnetic wave velocities in Table 1.

The signature response for Cenco Sealstix cement at a depth of 1.88 meters is shown in Figure 10. The signature response velocity is 1.7208*10^8 meter/second in the medium. The response shown in Figure 10 is the response to a pulse in the pulse-train impinging the surface of the half-space at time equal to -9.7254 nanosecond. One can verify this by the following calculation.

$$\begin{aligned}
f_{carrier} &= 2.1 \cdot 10^9 cycles/\sec \\
v_{air} &= 2.998 \cdot 10^8\ m/\sec \\
depth &= 1.88\ m \\
time_{air} &= \frac{depth}{v_{air}} = \frac{1.88}{2.998 \cdot 10^8} = 6.2708 \cdot 10^{-9} \sec
\end{aligned}$$

It takes $6.2708*10^{-9}$ seconds to travel 1.88 meters in a vacuum. However, in Cenco cement the waveform travels at only $1.7208*10^{8}$ meter/second. Therefore the time a pulse launched at the surface requires to reach a depth of 1.88 meters is approximately

$$time_{medium} = \frac{depth}{v_{medium}} = \frac{1.88}{1.7208 \cdot 10^{8}} = 10.925 \cdot 10^{-9} \text{ sec}$$

The reported pulse is shown to arise at approximately 1.2 nanoseconds, and we know that this pulse impinged upon the medium surface at time -9.7254 nanoseconds. These velocity considerations are important as they allow numerical computation in a temporal window starting at zero and ending at 10 nanoseconds. For figures 10-16, subtracting multiples of 9.7254 nanoseconds from the arrival time in table 1 will provide the correct time shown in the plots.

DII Material	Relative Dielectric Value at 2.1 GHz	Approximate Velocity in Medium (m/sec)	Approximate Arrival Time (nsec) At 1.88 Meters In Medium
Cenco Sealstix cement	3.0354	1.7208E+08	10.9254
Single Leaf foliage	22.7562	6.2847E+07	29.9141
Loamy soil 2.2% M.C.	3.6673	1.5655E+08	12.0088
Loamy soil 0.0% M.C.	2.4060	1.9328E+08	9.7269
Douglas Fir plywood	1.6185	2.3565E+08	7.9778
Royalgray paper	2.5301	1.8848E+08	9.9747
Lucite HM-122 plastic	2.5738	1.8687E+08	10.0604

Table 1. Approximate velocity of a 2.1 GHz square-wave modulated sinusoid pulse and the time the propagated wave takes to arrive at 1.88 meters depth in each medium.

Figure 9 is one period of a pulse train that recurs periodically every 9.5238 nanoseconds with the incoming pulse entering the medium at the beginning of each period. Table 1 shows that only Douglas fir plywood has an arrival time of less than one period. For all the other media, except for single leafy foliage, the plotted transmitted pulses entered the media at the beginning of the previous period. Higher water content causes foliage to have a smaller velocity and arrive much later. The plotted wave for foliage entered the medium three periods earlier.

A survey of the waveforms of the transmitted waves in the media shows major differences. Velocity differences have been discussed above. The formations of precursors around the first and last sinusoids of each pulse occur at different rates in the materials studied. The field strength in volts per meter of the precursors and of the central sinusoids of a pulse varies by up to a 20 to 1 ratio. The temporal duration at the base of the precursors varies with the rate of precursor formation at a given depth. These differences can be used to identify materials since they are also observed in waves reflected from the medium surface.

The signature responses of each of the media are shown in figures 10 to 16.

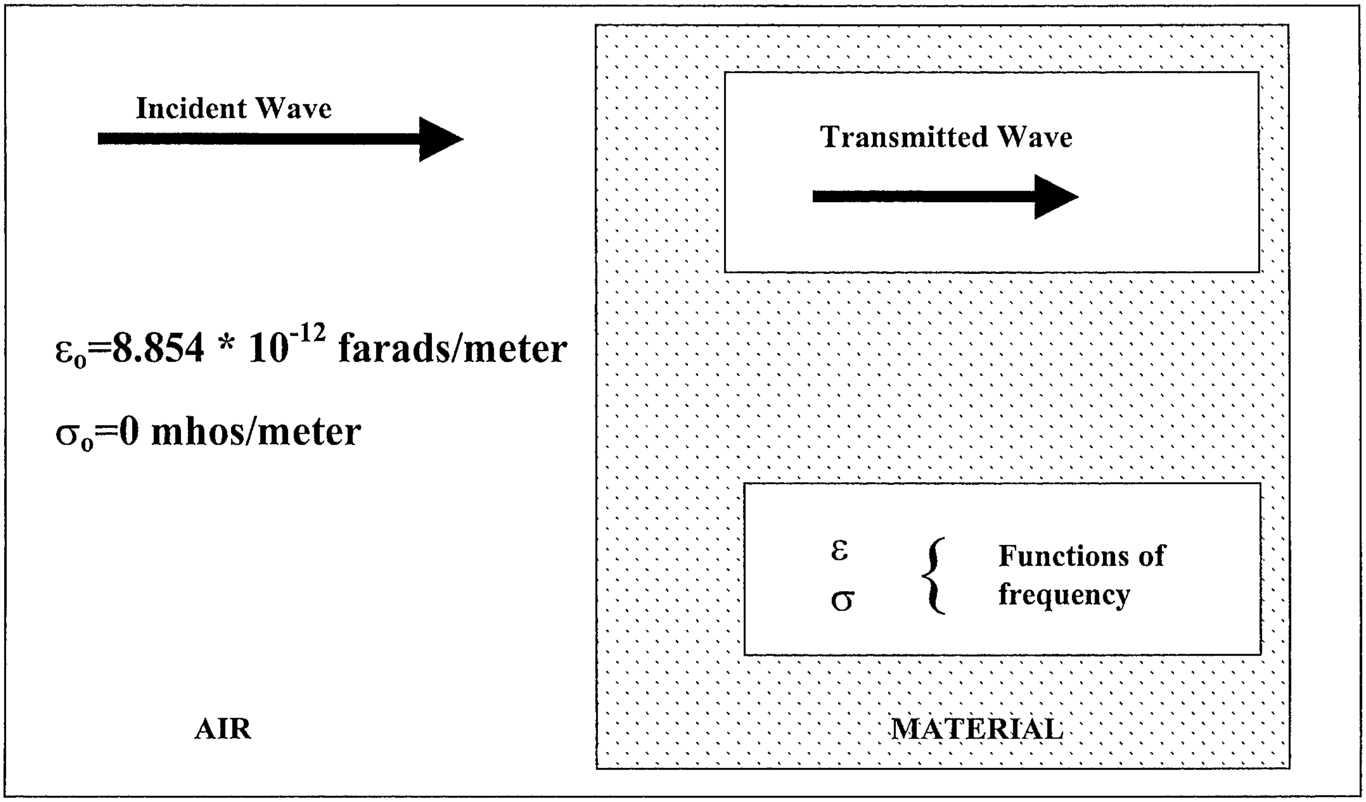

Figure 8. The half-space geometry studied in this paper.

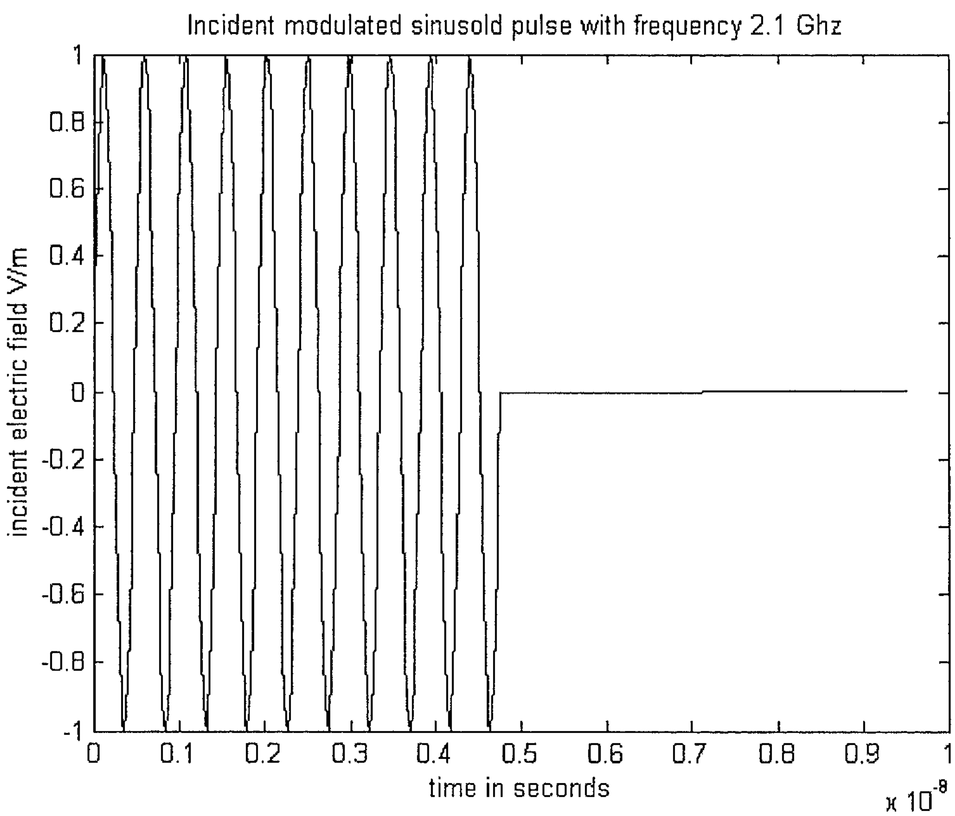

Figure 9. The pulse is a square-wave modulated sinusoid with 2.1 Ghz.

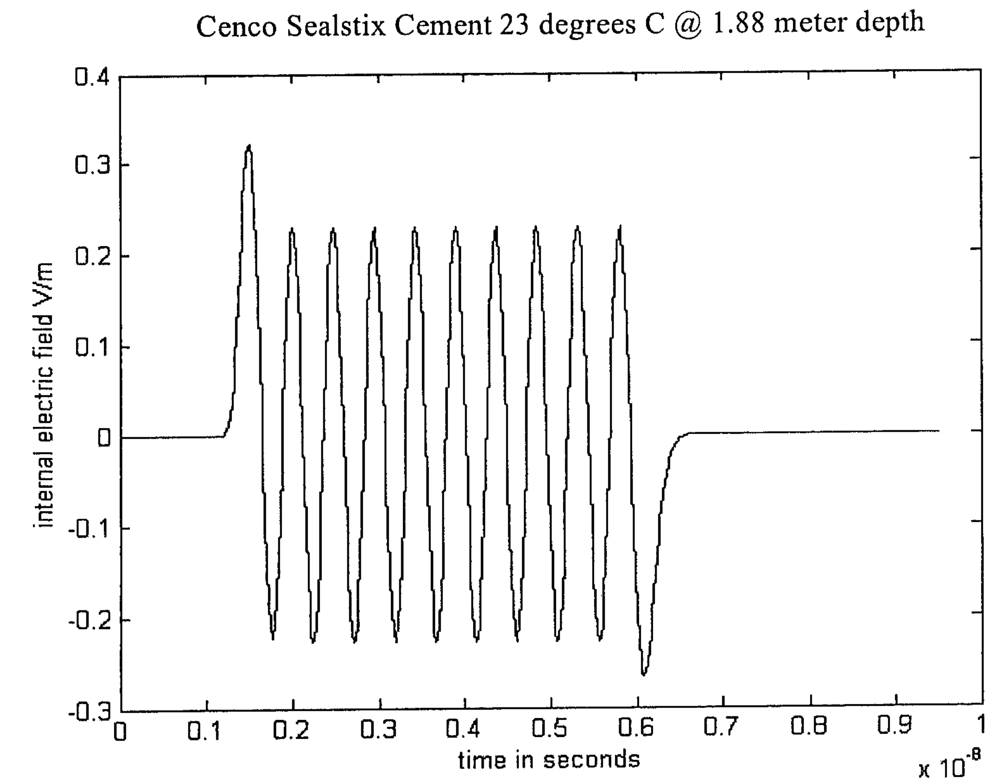

Figure 10. The response at 1.88 meter depth to the incident pulse shown in Figure 9 for Cenco Sealstix cement.

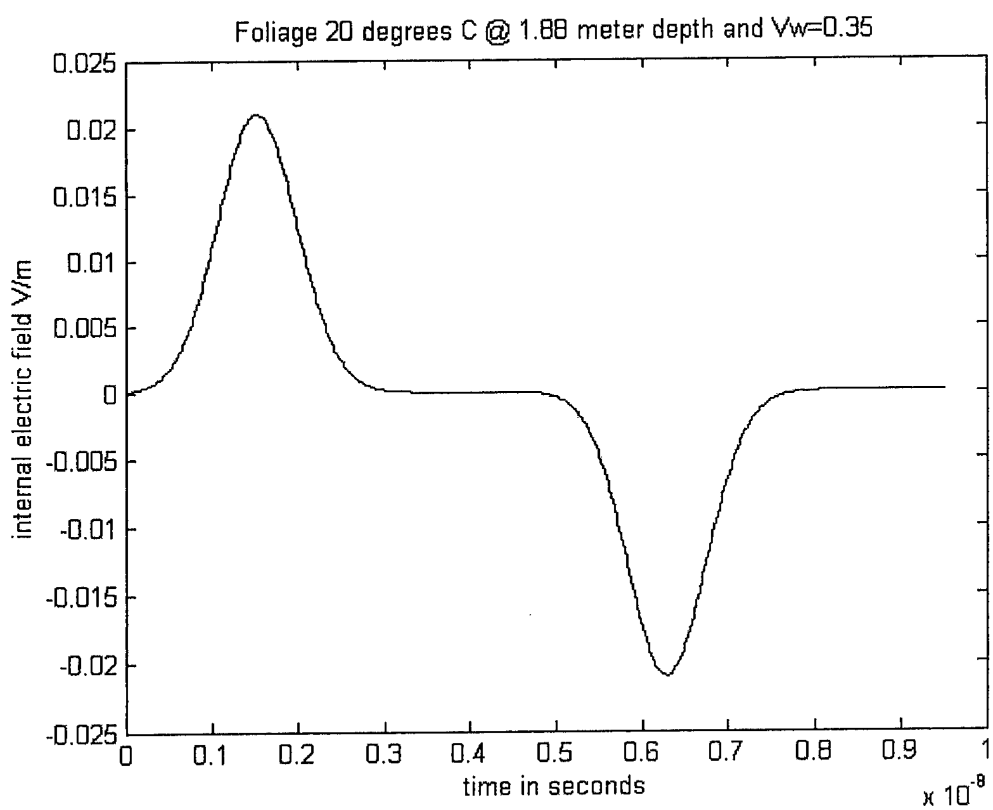

Figure 11. The response at 1.88 meter depth to the incident pulse shown in Figure 9 for Single leaf foliage.

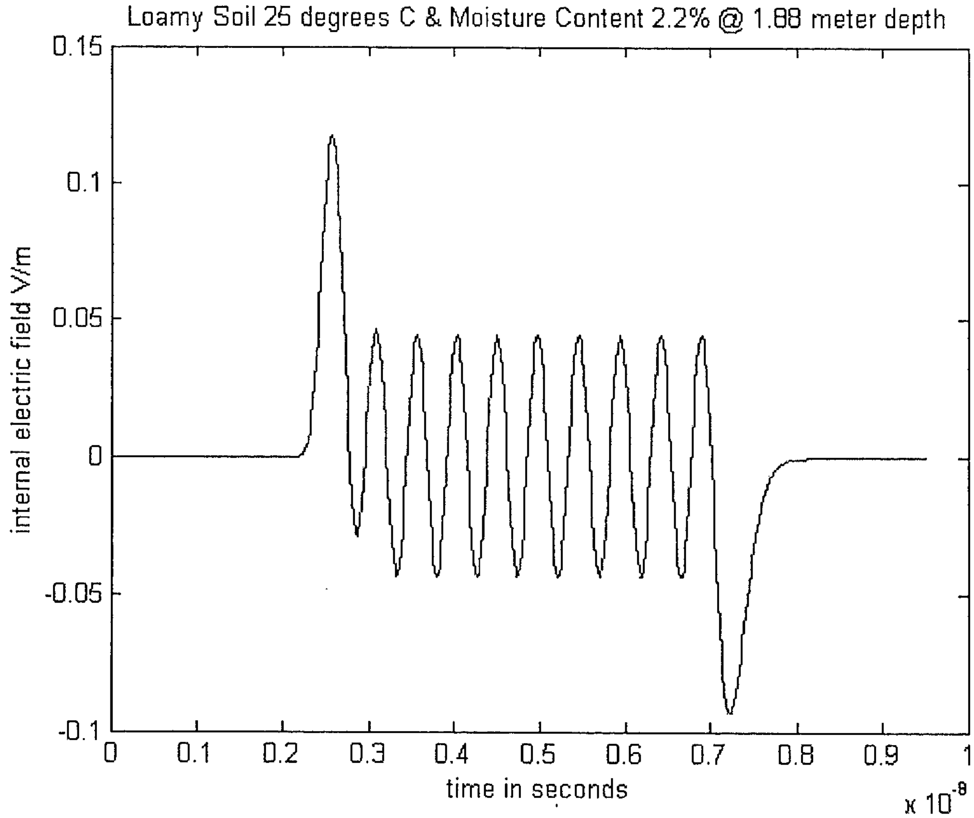

Figure 12. The response at 1.88 meter depth to the incident pulse shown in Figure 9 for Loamy soil 2.2% moisture content.

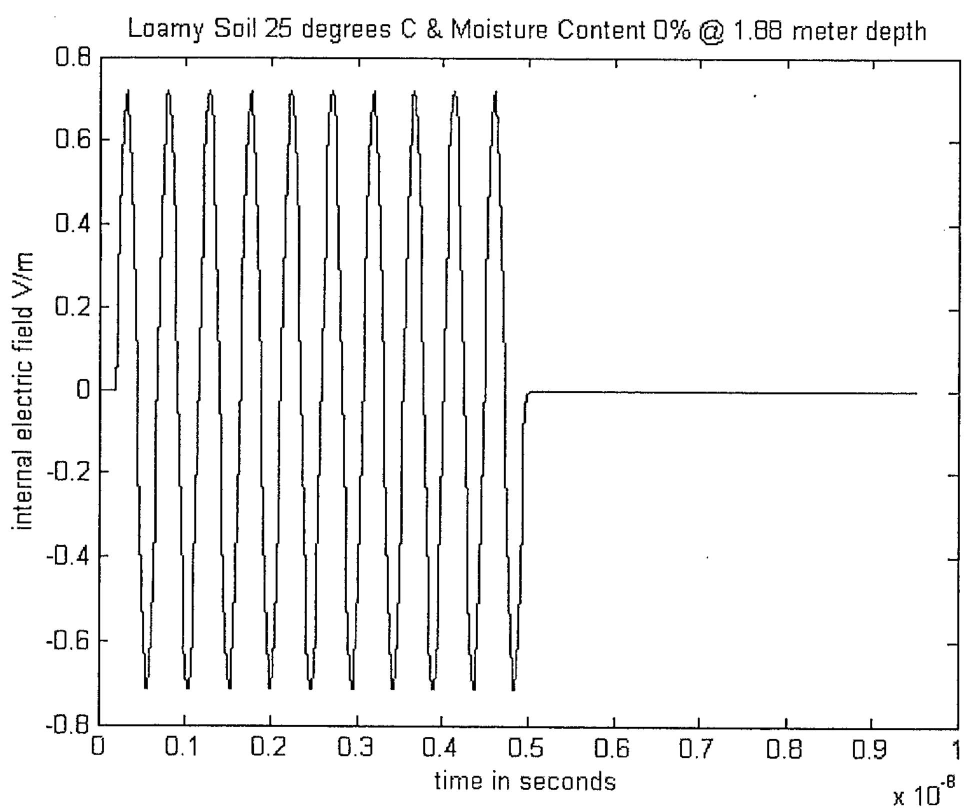

Figure 13 The response at 1.88 meter depth to the incident pulse shown in Figure 9 for Loamy soil 0.0% moisture content.

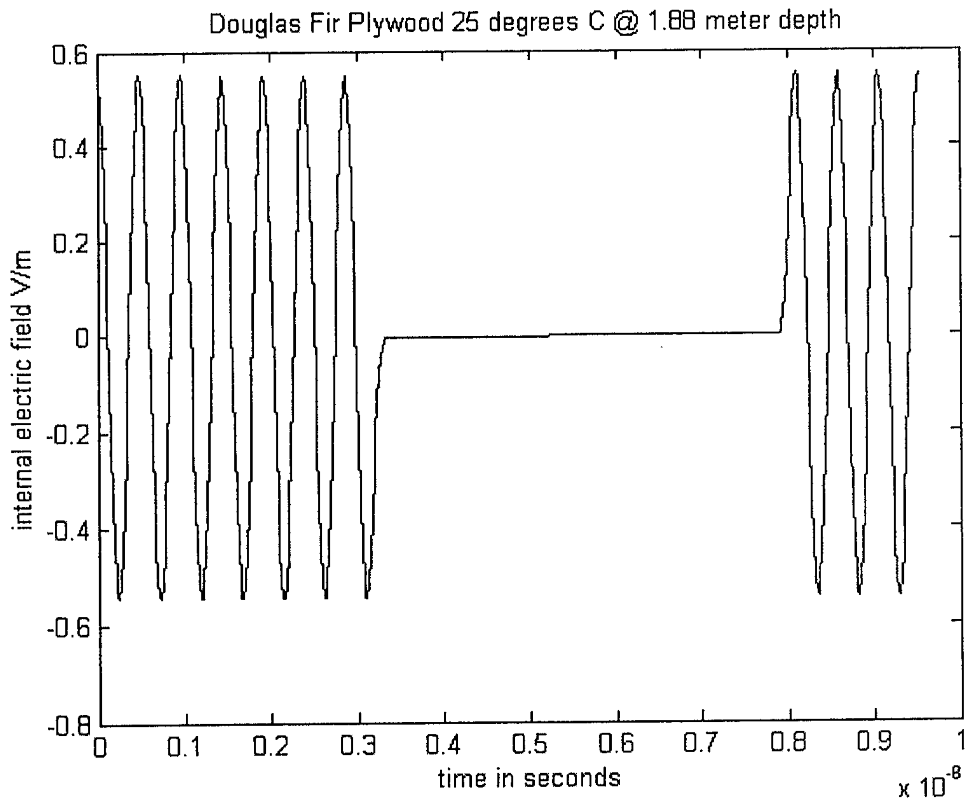

Figure 14 The response at 1.88 meter depth to the incident pulse shown in Figure 9 for Douglas Fir Plywood.

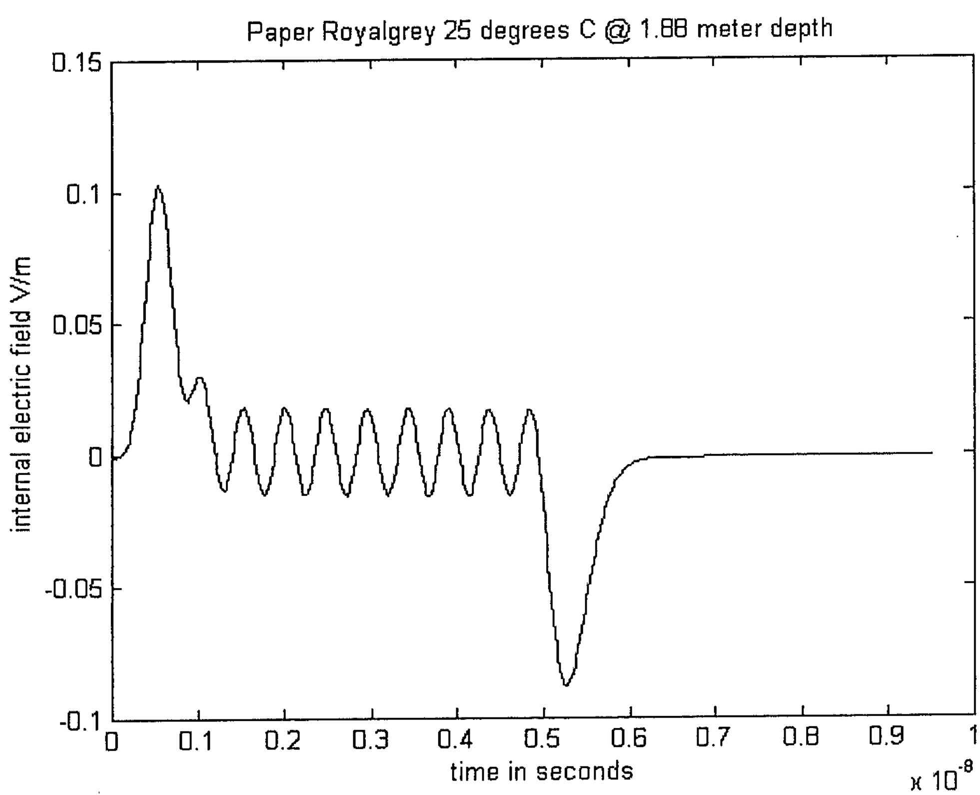

Figure 15 The response at 1.88 meter depth to the incident pulse shown in Figure 9 for Royalgrey paper.

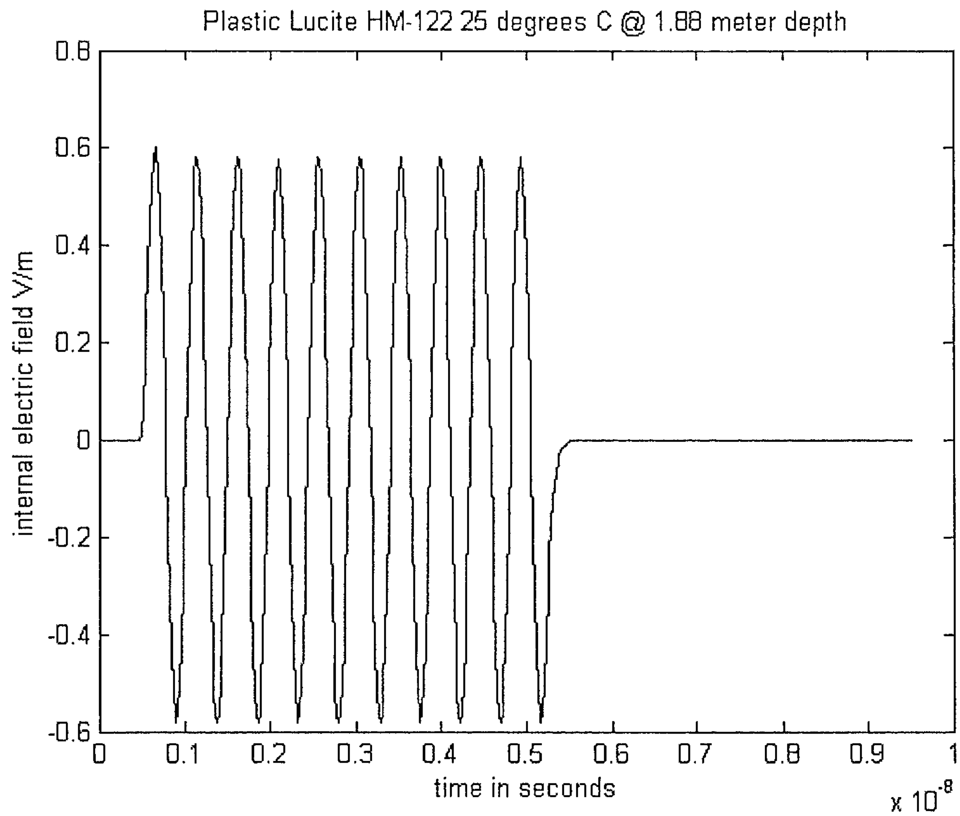

Figure 16 The response at 1.88 meter depth to the incident pulse shown in Figure 9 for Plastic Lucite Hm-122.

5 Summary

Dielectric values and conductivity data are needed to compute precursor formation in different materials. Our research group has collected some of this needed data for soil, foliage, cement, wood, paper, plastics, metals and water. For each material the following data were collected: name of material, relative dielectric value, loss tangent, frequency, temperature, moisture content and source of the data.

Material data came from published articles and were in several formats including tables, plots and fitted expressions. A common practice seems to be to linearly interpolate tabulated data for the dielectric value and conductivity rather than consider the inherent dependence of the two terms of the complex permittivity on each other to provide electromagnetic causality. A program developed in-house that considers the inherent dependence of the terms in the complex permittivity was used to fit multiple-term Debye-type expressions to published data.

A preliminary investigation was conducted on the materials mentioned above to see the existence of differences in waveform or precursor formation. A homogenous half-space was used to represent each material, the source was a square wave modulated pulse train with a carrier frequency of 2.1 GHz and measured at a depth of 1.88 meters from the boundary of the air-material model. The model predicts the characteristic of the waveform at the specified depth and frequency. Widely varying velocities in the medium were reported.

The data in this report suggest that scatter data may be used to identify materials. Additional work is needed to further investigate this result with experimental measurements and also to study the effects due to a non-homogeneous material.

Future work will extend the material database and improve causal model fitting.

Reference

(1). W. D. Hurt, J. M. Ziriax, P. A. Mason; "Variability in EMF Permittivity Values: Implications for SAR Calculations," IEEE Trans. on Biomedical Engineering, Vol. 47, No. 3, pp. 396-401, Mar 2000.

(2). W. D. Hurt; "Multiterm Debye Dispersion Relations for Permittivity of Muscle," IEEE Trans. on Biomedical Engineering, Vol. BME-32, No. 1, pp. 60-64, Jan 1985.

(3). J. A. Stratton; Electromagnetic Theory, McGraw-Hill Book Company, New York and London, page 605,1941.

(4). A. von Hippel; "Tables of Dielectric Materials Volume III," Laboratory for Insulation Research, Massachusetts Institute of Technology, Cambridge, Mass., O.N.R. Contract N5ori-78 T.O.1, June 1948.

(5). A. K. Fung, F. T. Ulaby; "A Scatter Model for Leafy Vegetation," IEEE Trans. on Geoscience Electronics, Vol. GE-16, No. 4, pp 281-286, Oct 1978.

(6). W. R. Ting, S.O. Nelson; "Dielectric Properties of Materials for Microwave Processing-Tabulated," Journal of Microwave Power, 8(1), pp23-65, 1973.

(7). M. A. EL-Rayes, F. T. Ulaby; "Microwave Dielectric Spectrum of Vegetation—Part I: Experimental Observations," IEEE Trans. on Geoscience and Remote Sensing, Vol. GE-25, No. 5, Sept. 1987.

(8). J. A. Stratton; Electromagnetic Theory, McGraw-Hill Book Company, New York and London, page 275,1941.

Appendix A
Measured relative dielectric value and conductivity data

Frequency (Hertz)	Steel ε_r	Steel σ(Siemens/meter)	Cement (C. S.) ε_r	Cement (C. S.) σ(Siemens/meter)
1e2	1	0.5e7	3.90	9.81e-10
1e3	1	0.5e7	3.75	6.99e-9
1e4	1	0.5e7	3.55	5.43e-8
1e5	1	0.5e7	3.37	4.50e-7
1e6	1	0.5e7	3.23	4.31e-6
1e7	1	0.5e7	3.13	4.74e-5
1e8	1	0.5e7	------------	------------
3e8	1	0.5e7	------------	------------
3e9	1	0.5e7	2.96	1.04e-2
1e10	1	0.5e7	------------	------------
2.5e10	1	0.5e7	------------	------------

Reference (3)
σ range from
0.5e7-1.e7 S/m
at 20C

Reference (4)
Cenco Sealstix
(C. S.) at 23C

Frequency (Hertz)	Loamy Soil 0.0 % ε_r	Loamy Soil 0.0 % σ(Siemens/meter)	Loamy Soil 2.2 % ε_r	Loamy Soil 2.2 % σ(Siemens/meter)
1e2	----------	----------	----------	----------
1e3	----------	----------	----------	----------
1e4	2.69	5.23e-8	18.0	1.60e-5
1e5	2.60	4.34e-7	----------	----------
1e6	2.53	2.56e-6	6.9	2.50e-4
1e7	2.48	1.95e-5	4.0	1.00e-3
1e8	----------	----------	----------	----------
3e8	2.47	2.67e-4	3.5	3.50e-3
3e9	2.44	4.84e-4	3.5	2.34e-2
1e10	2.44	1.89e-3	3.5	5.84e-2
2.5e10	----------	----------	----------	----------

Reference (6)
0.0% water by
weight at 25C

Reference (6)
2.2% water by
weight at 25C

Frequency (Hertz)	Fir Douglas Plywood		Royalgrey paper	
	ε_r	σ(Siemens/meter)	ε_r	σ(Siemens/meter)
1e2	2.1	1.34e-10	3.30	1.06e-10
1e3	2.1	1.23e-9	3.29	1.41e-9
1e4	2.05	1.48e-8	3.22	2.10e-8
1e5	1.95	1.84e-7	3.10	3.45e-7
1e6	1.9	2.43e-6	2.99	6.32e-6
1e7	1.8	3.20e-5	2.86	9.07e-5
1e8	----------------------		2.77	1.02e-3
3e8	1.7	1.02e-3	2.75	3.03e-3
3e9	----------------------		2.70	2.52e-2
1e10	----------------------		2.62	5.87e-2
2.5e10	1.6	4.90e-2	----------------------	
	Reference (4) at 25C		Reference (4) at 25C	

Frequency (Hertz)	Plastic Lucite HM-122 ε_r	σ(Siemens/meter)
1e2	3.18	9.91e-10
1e3	2.95	6.89e-9
1e4	2.81	4.53e-8
1e5	2.75	3.06e-7
1e6	2.68	2.09e-6
1e7	2.62	1.31e-5
1e8	2.60	8.68e-5
3e8	2.59	2.33e-4
3e9	2.57	2.06e-3
1e10	2.57	5.86e-3
2.5e10	2.56	8.54e-3

Reference (4) at
25C